Cross Sections for Ion and Electron Production in Gases by 0.15–1.00-MeV Hydrogen and Helium Ions and Atoms*

L. J. Puckett,† G. O. Taylor, and D. W. Martin
School of Physics, Georgia Institute of Technology, Atlanta, Georgia 30332
(Received 14 October 1968)

Reported in this paper are the measurements of absolute total apparent cross sections for processes leading to slow electron and ion production in the gases He, Ar, H_2, and N_2 by incident beams of He^{++}, He^0, and H^0 in the energy range 0.15 to 1.00 MeV. From these measurements absolute total apparent cross sections for ionization, electron capture, and stripping were deduced. The present results are compared with those from other experiments and with available theoretical calculations.

I. INTRODUCTION

The work described herein constitutes a segment of a continuing program in this Laboratory of absolute determinations of the cross sections for ion and electron production in atomic and molecular gases by various high-energy ions and atoms. The results for protons and He^+ have been previously reported.[1,2] Some limited early results[2] for He^{++} over a reduced energy range are revised and extended in the present paper to cover the total energy range of the accelerator used. A detailed comparison of the previous results with the available theoretical calculations has also been published.[3,4]

Reported in the present paper are cross section measurements and comparisons with theory for He^0 and He^{++} projectiles over the energy range 0.15 to 1.00 MeV, as well as for H^0 projectiles from 0.15 to 0.40 MeV.

Three types of collision processes contribute to the total production cross sections reported here: (a) ionization – the ejection of free electrons from the target, (b) capture – the capture by the projectiles of one or more electrons from the target, and (c) stripping – the ejection of free electrons from the projectile.

The multiplicity of events that can occur in high-energy collision is illustrated for the case of fast hydrogen atoms incident on helium in Eqs. (1)–(5). Reactions leading to the formation of negative ions are omitted because of their small relative contribution in the energy range of this work. For heavier target gases such as argon, of course, the number of possible types of events is even more numerous, because of the larger number of electrons that may be affected by the collision. A still further increase in the multiplicity of events arises when molecular targets are used, and the reaction products may include dissociation fragments that are singly or multiply ionized.

Reactants	Reaction products	Cross section	
$H^0 + He^0$	$\rightarrow H^0 + He^+ + e$	${}_{00}\sigma_{01}$	(1)
	$\rightarrow H^0 + He^{++} + 2e$	${}_{00}\sigma_{02}$	(2)
	$\rightarrow H^+ + He^0 + e$	${}_{00}\sigma_{10}$	(3)
	$\rightarrow H^+ + He^+ + 2e$	${}_{00}\sigma_{11}$	(4)
	$\rightarrow H^+ + He^{++} + 3e$	${}_{00}\sigma_{12}$.	(5)

By the definitions adopted here, Reactions (1) and (2) are called simple ionization events, single and double, respectively. Reaction (3) is a simple stripping event.

The cross-section notation of Hasted,[5] shown in the right-hand column of the list of Eqs. (1)–(5), is arranged to convey all the information concerning the reaction process that is contained in the reaction equation. The symbols ${}_{ab}\sigma_{ij}$ represent the cross section for a projectile of charge a, incident on a target of charge b, to undergo a reaction that leads to a final state of the projectile of charge i, and of the target, of charge j. In this experiment some of these processes are indistinguishable, e.g., Reactions (1) and (2) above. When such is the case, it is indicated in a given reaction by leaving the subscript unspecified.

Measurement of the cross sections characterizing the three fundamental reactions of electron capture, stripping, and ionization may be divided into two major categories as follows: (a) observation of the charge states of the fast beam particles after they emerge from the collision region, and (b) observation of the residual slow particles formed in the collision events.

Most experiments concerned with the measurement of the electron capture and stripping cross sections have been of type (a) while all experiments for the measurement of ionization cross sections are necessarily of type (b). As will be seen later, measurements of type (b), such as are reported here, can often be used to obtain information on the stripping and electron capture cross sections.

In this investigation only "thin-target" methods have been used. The analysis of the slow collision

products (i.e., all collision fragments other than the scattered fast projectile) consisted simply of their collection to planar electrodes by a transverse electric field, and measurement of the resulting electrode current.[1,2] The quantities directly measured are the apparent cross sections for the production of slow positive ions, σ_+, and of electrons, σ_-. For the case of neutral H atoms incident on helium

$$\sigma_+ = {}_{00}\sigma_{01} + {}_{00}\sigma_{11} + 2({}_{00}\sigma_{02} + {}_{00}\sigma_{12}) , \quad (6)$$

$$\sigma_- = {}_{00}\sigma_{01} + {}_{00}\sigma_{10} + 2({}_{00}\sigma_{02} + {}_{00}\sigma_{11}) + 3\,{}_{00}\sigma_{12} , \quad (7)$$

$$\sigma_- - \sigma_+ = {}_{00}\sigma_{10} + {}_{00}\sigma_{11} + {}_{00}\sigma_{12} , \quad (8)$$

with corresponding equations differing in detail for the cases of other projectiles and/or targets.

In keeping with accepted usage, we define the apparent total ionization cross section σ_i to be the sum of the cross sections for all processes involving the production of a singly-charged slow ion pair, plus twice the cross sections for processes producing a doubly-charged slow ion pair (e.g., a doubly-charged positive ion and two free electrons), and so forth for more highly charged ion pairs. This definition excludes from σ_i all of the *simple* stripping or capture processes, single or multiple, but includes combination events like Eq. (4) or (5). Similarly, we define the apparent stripping (or capture) cross section σ_s (or σ_c) to be the sum of the cross sections for all processes in which one electron is stripped from (captured by) the fast projectile, plus twice the cross sections for stripping (capture) of two electrons, etc. A multiple combination event such as Eq. (5) is thus counted once in σ_s and twice in σ_i.

With these definitions, we can write Eqs. (6)–(8), respectively, for the present case of neutral H atoms incident on helium, as

$$\sigma_+ = \sigma_i , \quad (9)$$

$$\sigma_- = \sigma_i + \sigma_s , \quad (10)$$

$$\text{and } \sigma_- - \sigma_+ = \sigma_s . \quad (11)$$

For the more general case, however, where electron capture processes are important, these equations become

$$\sigma_+ = \sigma_i + \sigma_c , \quad (12)$$

$$\sigma_- = \sigma_i + \sigma_s , \quad (13)$$

$$\text{and } \sigma_- - \sigma_+ = \sigma_s - \sigma_c . \quad (14)$$

By means of these relations, σ_i and σ_s or σ_c have been determined from the measured σ_+ and σ_-, for the projectiles He^{++}, He^0, and H^0 on the target gases He, Ar, H_2, and N_2.

II. EXPERIMENTAL APPARATUS AND TECHNIQUES

Beams of H^+ and He^+ in the energy range from 0.15 to 1.00 MeV were obtained directly from a Van de Graaff accelerator, and were converted to the H^0, He^0, and He^{++} projectiles used in this experiment through charge changing collisions in a gas cell. The basic apparatus and measurement techniques are similar to those described by Langley *et al.*,[2] with certain detailed modifications as set forth below.

The selection of the gas used in this cell was based on the equilibrium fractions[6] of the various beam components. It was determined that, in this energy range, the gas that produced the largest fractions of He^0 and H^0 was helium. Similarly, for the production of He^{++}, molecular nitrogen was indicated.

The mixed beam of fast particles in various charge states emerging from the gas cell was separated according to charge in a parallel-plate electrostatic analyzer. In order that the separated beam not become contaminated with other charge states in further charge changing collisions, it was essential to confine the high pressure to the region of the gas cell as much as practicable; for this purpose separately pumped chambers were installed outside both ends of the gas cell, and a quite satisfactory pressure reduction of about 10^5 between the gas cell and the remainder of the system was achieved.

A schematic view of the modified collision chamber and its entrance collimator is given in Fig. 1. The selected beam emerging from the electrostatic analyzer was passed through the three-slit collimator, designed to minimize the contamination of the beam with particles scattered from slit edges. The beam incident on the collimator was diverging from the exit aperture of the gas cell, some two meters away. The primary geometrical collimation of the diameter and divergence of the beam was therefore established by the first aperture "a," which was the smallest of the three. The second aperture "b" was large enough not to further intercept the main beam defined by the preceding apertures. Its function was to intercept particles scattered from the edge of the

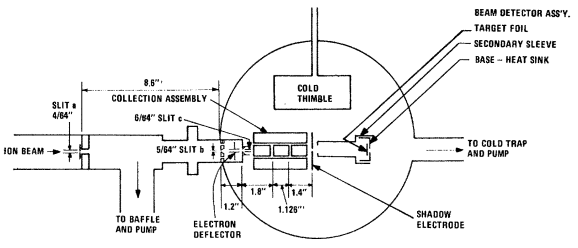

FIG. 1. Schematic view of the collision chamber, showing the multiple function beam detector assembly for either charged or neutral beams. The two planar arrays of slow-ion collection electrodes, one of which is shown here rotated parallel to the plane of the page, are actually oriented perpendicular to the page, so that the collision region is concealed from the cold thimble.

first aperture and from the residual gas, but its own edge was kept clear of the main beam so as not to serve as a further source of such scattered particles. The third and last aperture, "c," was the largest in diameter of the three, but was a cylindrical channel to reduce its gas conductance, and it served to define the boundary between the evacuated beam tube and the target gas in the collision chamber. The region between the second and third apertures was evacuated to less than $\frac{1}{5}$ of the target gas pressure, and it was expected that a negligible number of charge changing gas collisions occurred in the collimator.

Among the scattered particles of concern here were first, of course, fast heavy beam particles which, having suffered a scattering collision, might also have suffered a change in their charge, so that they would now represent a contaminant in the beam. Also important in these measurements were fast "knock-on" electrons traveling with the beam, with speeds of the same order of magnitude as the heavy particles. Previous experience had shown that such electrons, entering the collision chamber with the beam, could be most troublesome in the measurement of σ_-. A small pair of electrostatic deflector plates was installed in the region between the second and third apertures to deflect away from the last aperture any such electrons in the beam. Application of up to 600 V to this deflector, calculated to be more than enough to deflect out electrons with the same velocity as the heavy beam particles, was found to have no noticeable effect on the electron current collected from the measurement region, or on the saturation curves for this current. It was concluded from this that the geometrical design of the collimator has essentially eliminated the previously troublesome problem of fast electrons in the beam.

The target-gas pressure in the collision chamber was sufficiently low that "thin-target" conditions prevailed. The slow positive ions and electrons produced in the target gas were collected by two oppositely charged parallel-plate assemblies[2] mounted parallel to and on opposite sides of the beam axis. The current to only the center electrode of each array, collected from a well defined region of the target gas, was included in the measurements. (The plane of the array of collection electrodes shown in Fig. 1 was actually at right angles to the plane of the figure, rather than as shown.)

In order to reduce the ionization currents from the background gas to acceptable levels, it was found necessary to install a liquid nitrogen thimble inside the collision chamber. It was, however, so positioned that it could not be directly "seen" from any point along the beam path in order to avoid a serious temperature perturbation of the gas in the collision region. Cross-section measurements with the trap at room temperature and at liquid nitrogen temperature showed no temperature dependence, after correction of the room-temperature results for the large background gas ionization. The base vacuum in the collision chamber with the trap cold was less than 1×10^{-7} Torr, and in this condition, the contributions to the measured cross sections from the background were always less than one percent of the total cross sections.

The target-gas pressure between the collector electrodes was measured with a liquid-nitrogen-trapped McLeod gauge, which will be further discussed.

The beam detector (shown in Fig. 1) was designed and used in this investigation to trap the beam totally and to provide at will for any of three observations: (1) the net current delivered by the beam to the entire collector assembly; (2) secondary emission current from the beam target foil, collected on the sleeve; and (3) total power of the beam, obtained through observation of the temperature rise of the thermally isolated target foil, by means of a thermocouple. The latter two functions were provided for the detection of neutral beams. One thermocouple junction was spot-welded to the back of the target foil and the other was attached to the heat sink, which served as the reference temperature.

Considerable care was taken in the design of this neutral beam detector in order to obtain both a satisfactory sensitivity, which was dictated by the low neutral beam intensity, and to produce a reasonable response time, which in turn was dictated by the rate of fluctuation of the beam intensity. The detector sensitivity and response time can be changed by varying the material and diameter, and hence the thermal conductivity of the wires supporting the foil. The values selected for this experiment provided a sensitivity of 3°C/mW, or in terms of thermocouple emf, about 0.1 V/W, with a time constant of about 13 sec. Further details of the detector can be found in a report by Puckett *et al.*[7]

The thermal function of the detector was calibrated by using first a beam of singly charged particles, for which the emf response of the thermocouple was verified to be directly proportional within the range of this experiment to the total beam power impinging on the foil. The latter was given for the charged beam by the product of the Van de Graaff voltage and the net beam current as measured by function #1. One then obtained the "current" of a neutral beam as the product of this same proportionality constant and the observed emf, divided by the accelerator voltage. The secondary emission function of this detector had been provided as a fast-response indication of neutral beams, but was used only for an intermediate step in the calibration procedure.

In a calibration of this type, it was necessary to assure that the singly charged ion beam used was not appreciably contaminated with neutral particles, and when performing cross-section measurements with the neutral beams, it was similarly necessary

to assure that the neutral beam was not appreciably contaminated with charged particles. Tests indicated that in both cases the contamination of the beams was only about 0.1%, which in this experiment was negligible.

Before using the apparatus to measure new cross sections it was verified that both the ion and electron currents in the collision chamber saturated as the collection field was increased.

As an overall check of the apparatus and procedures, the measurements of σ_+ and σ_- by Hooper[3] for H^+ on Ar were repeated using collection potentials of 350 V. The present results were within two percent of those average values obtained by Hooper over the energy range from 0.3 to 1.0 MeV. It was observed that in the upper energy range $\sigma_+ = \sigma_-$, which implies that the electron capture cross section is completely negligible in comparison. This result is in accordance with the measurements of Barnett *et al.*[8] With this excellent agreement, the apparatus was considered to be sufficiently tested to produce reliable results.

The estimated maximum measurement errors, with the exception of the systematic McLeod gauge errors, are listed in Table I.

TABLE I. Estimated maximum errors (%) in σ_+ and σ_- from all sources except for McLeod gauge errors.

Measured quantities	Projectiles He^{++}	He^0	H^0
Slow ion or electron current	± 2	± 2	± 2
He^{++} beam current	± 2	• • •	• • •
(He^0, H^0) beam power	• • •	± 2	± 7
Detector calibration	• • •	± 5	± 5
Gas pressure (random)	± 1	± 1	± 1
Totals (cross-section errors)	± 5	± 10	± 19

The only appreciable systematic errors believed[7] to be associated with the McLeod gauge used are those due to the Gaede effect.[9] From recent work[10–15] it appears that the magnitude of these errors may in practice be substantially less than the theoretically computed values, depending upon the degree of cleanliness of the exposed mercury surface and the distributed source of mercury along the wall of the tubulation. Because of the uncertainty in the actual magnitude of the effect, the present cross-section results are presented without correction for the Gaede effect. If, however, the full theoretical correction[7] for this effect were applied to our McLeod gauge, then the presently reported cross sections would be revised downward for each of the four target gases as follows:

H_2 – 2%, He – 3%, N_2 – 11%, and Ar – 13%.

III. PRESENT RESULTS AND COMPARISONS WITH OTHER EXPERIMENTAL AND THEORETICAL RESULTS

A. He^{++} Ion Beams

Presented in Table II and Figs. 2–5 are the measured total apparent cross sections for the production of positive ions σ_+ and electrons σ_- by fast doubly charged helium ions in targets of helium, argon, hydrogen, and nitrogen, respectively. The estimated experimental uncertainties are as stated above in Table I.

For the He^{++} projectile, σ_S is zero, so from Eqs. (13) and (14), σ_- is the total apparent ionization cross section σ_i, and the difference $(\sigma_+ - \sigma_-)$ is the total apparent electron capture cross section σ_c. The present values of the latter quantity from

TABLE II. Apparent cross sections for production of positive ions σ_+ and electrons σ_- by an incident beam of He^{++} (All cross sections are in units of 10^{-16} cm^2 per molecule.)

Projectile energy (keV)	Helium σ_+	Helium σ_-	Argon σ_+	Argon σ_-	Hydrogen σ_+	Hydrogen σ_-	Nitrogen σ_+	Nitrogen σ_-
180	5.55	1.37	• • •	• • •	• • •	• • •	25.2	13.7
200	5.50	1.55	26.3	16.3	11.7	6.20	24.5	14.3
250	4.98	1.93	24.3	16.8	10.5	6.70	23.2	14.9
300	4.61	2.21	22.6	17.2	9.35	6.85	21.4	15.0
350	4.28	2.44	21.4	17.3	8.65	6.97	20.4	15.2
400	3.93	2.47	20.4	17.3	7.92	6.85	19.4	15.2
500	3.48	2.51	18.7	16.7	6.90	6.34	17.9	14.9
600	3.12	2.50	17.5	16.2	6.20	5.90	16.3	14.3
700	2.84	2.43	16.5	15.6	5.61	5.37	15.2	13.7
800	2.61	2.30	15.5	14.9	5.01	4.91	14.3	13.2
900	2.40	2.19	14.8	14.3	4.67	4.59	13.5	12.7
1000	2.24	2.06	14.2	13.7	4.23	4.17	12.9	12.2

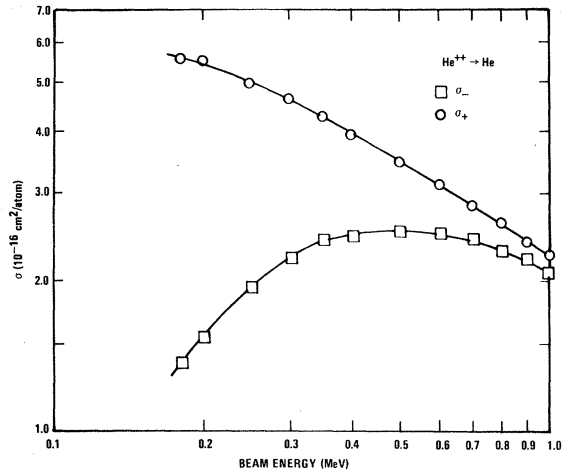

FIG. 2. He^{++} ions incident on He: The total apparent cross sections for the production of positive ions σ_+, and of free electrons σ_-.

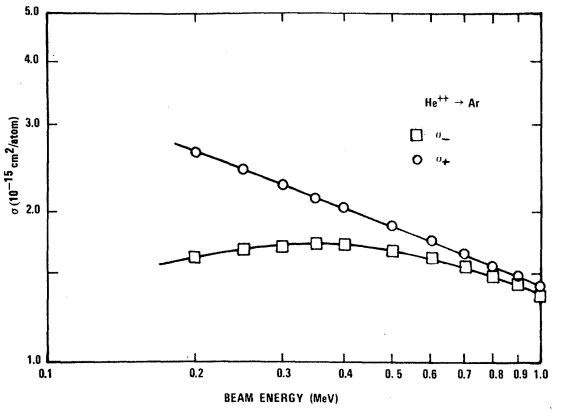

FIG. 3. He^{++} ions incident on Ar: The total apparent cross sections for the production of positive ions σ_+, and of free electrons σ_-.

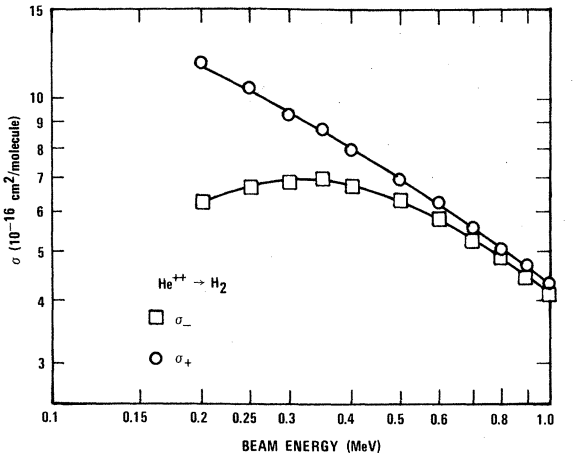

FIG. 4. He^{++} ions incident on H_2: The total apparent cross sections for the production of positive ions σ_+, and of free electrons σ_-.

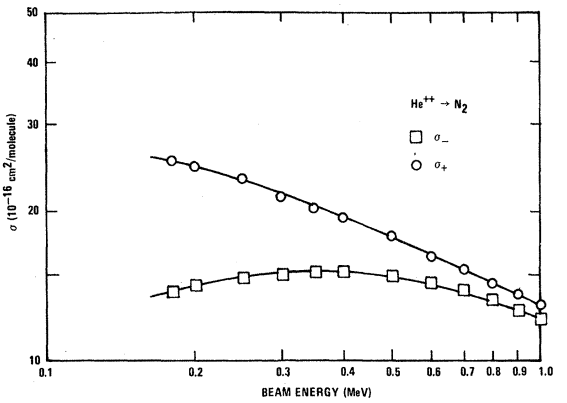

FIG. 5. He^{++} ions incident on N_2: The total apparent cross sections for the production of positive ions σ_+, and of free electrons σ_-.

the present measurements are presented separately for the same four cases in Figs. 6–9. A theoretical calculation of σ_c for the case of He^{++} incident on He by Fulton *et al.*[16] is shown in Fig. 6. Also shown for comparison are the experimental σ_c measurements of Pivovar *et al.*,[17] of Allison,[18] and of Nikolaev *et al.*[19] It should be noted that the experiments of all three of these latter groups of investigators are based upon the direct observation of the change in charge state of the fast beam particles, i.e., the experiments denoted as class (a) in Sec. I. Thus these experiments involved entirely different types of measurements from the present experiment, and had quite different sources of error.

The stated errors in the latter experiments were all about ±10%. Each of the groups, however, employed a McLeod gauge as a pressure standard, so that there were some additional uncertainties, not appreciated at the time, with regard to systematic errors. It may be noted that in some cases, the results of these workers, notably Pivovar and Allison, differ by as much as 75%, which is significantly outside of their stated combined error limits. The measurements made in this laboratory are seen to generally fall between those of Pivovar and of Allison, and agreement with Pivovar generally improves with increasing energy. This is a surprising observation because in the upper energy range our difference $(\sigma_+ - \sigma_-)$ becomes fractionally small compared with either σ_+ or σ_-, and, therefore, should become subject to larger errors than in σ_+ and σ_- individually. Specifically for He^{++} on H_2 the difference between σ_+ and σ_- at 1 MeV is only two percent, less than the observed random error of about ±3% in single determinations of the separate cross sections. The rather good agreement with Pivovar at this energy therefore serves to indicate that the present σ_+ and σ_- are determined relatively to better than one percent. The agreement with Pivovar

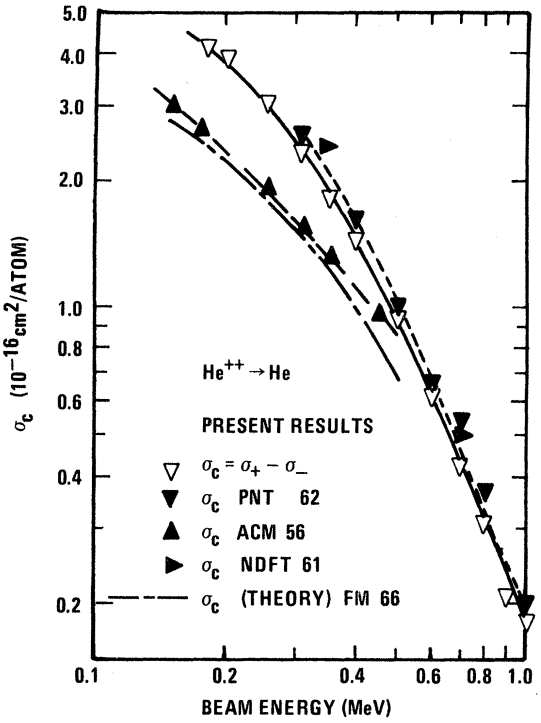

FIG. 6. He^{++} ions incident on He: The total apparent capture cross section σ_c. PNT 62: Pivovar *et al.* (Ref. 17); ACM 56: Allison *et al.* (Ref. 18); NDFT 61: Nikolaev *et al.* (Ref. 19); FM 66: Fulton and Mittleman (Ref. 16).

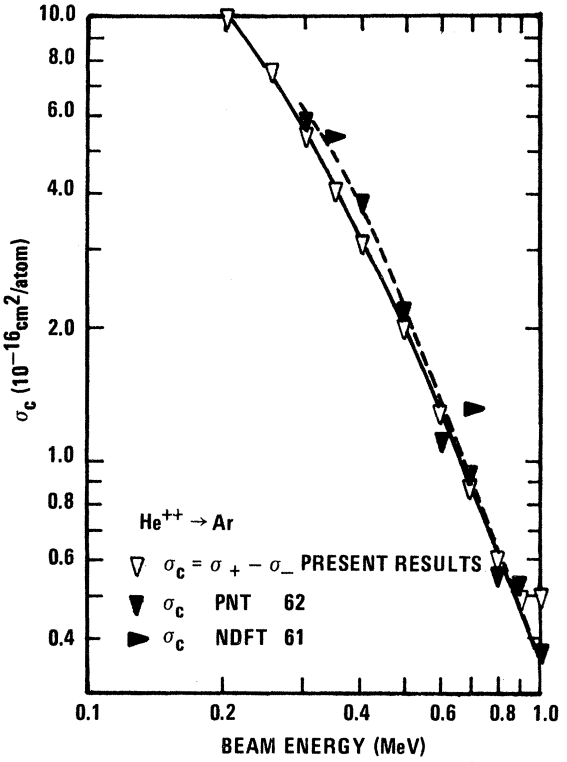

FIG. 7. He^{++} ions incident on Ar: The total apparent capture cross section σ_c. PNT 62: Pivovar *et al.* (Ref. 17); NDFT 61: Nikolaev *et al.* (Ref. 19).

provides strong confirmation of the validity of both the present total ion production measurements and the charge changing cross section measurements of Pivovar.

B. He^0 and H^0 Neutral Beams

A major concern in this experiment was the possibility that the fast neutral beams H^0 and He^0, since they were obtained through electron capture by H^+ and He^+ beams in the gas cell, might contain an appreciable fraction of atoms in excited states. The magnitudes and even the ratios of the cross sections for most types of collisions would be expected to be different for such excited atoms from those for ground-state atoms. To consider the possibility of atoms in excited states reaching the collision chamber, the flight time from the gas cell to the collision chamber may be compared to the lifetimes of such states. Using available calculations and measurements, which relate the lifetime to the principal quantum number n of the excited state for hydrogen[20] and for helium,[21] one finds that all allowed states of hydrogen with $n \leq 6$ and of helium with $n \leq 7$, are too short lived to survive the transit even at the highest beam velocities used here. A separate calculation[22] indicates that the probability of producing excited states with $n > 7$ does not exceed about 0.003. Therefore, it is not expected that ordinary states of "allowed" excitation can cause any difficulties in this experiment.

However, H^0 and He^0 both have low-lying metastable states which cannot decay by allowed transitions, and have sufficiently long lifetimes to reach the collision chamber. Consideration of such metastable states is included in the separate discussions of the H^0 and He^0 results that follow.

1. He^0 *Atom Beams*

The present results for the total apparent ion and electron production cross sections by fast incident neutral helium atoms in the four target gases helium, argon, hydrogen, and nitrogen are presented in Table III and Figs. 10–13. Also shown for comparison are the similar measurements of Solov'ev *et al.*,[23] for σ_+, which extend up to only 0.18 MeV, and agree well with the present results in the overlap region.

At these high energies, the probability is very small that neutral projectiles will capture electrons to form negative ions.[24] Therefore, from Eqs. (12) and (14) with $\sigma_c = 0$, σ_+ is identical to the total apparent ionization cross section σ_i. Similarly, the difference $(\sigma_- - \sigma_+)$ cross section is just the total apparent stripping cross section σ_s for the fast

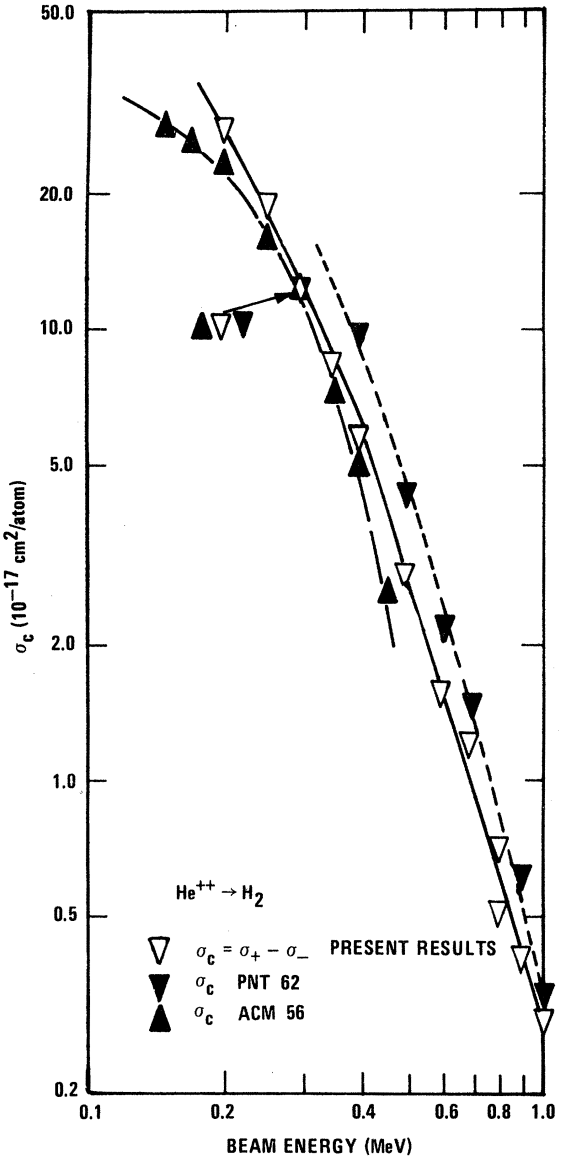

FIG. 8. He^{++} ions incident on H_2: The total apparent capture cross section σ_c. PNT 62: Pivovar *et al.* (Ref. 17); ACM 56: Allison *et al.* (Ref. 18).

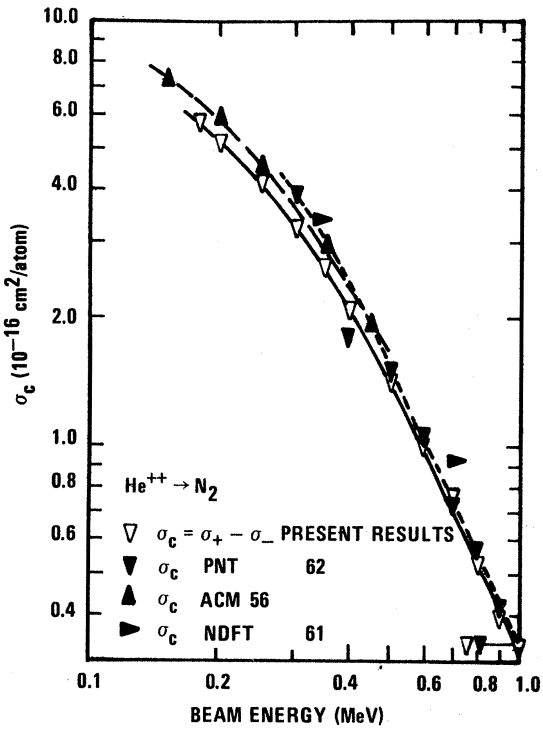

FIG. 9. He^{++} ions incident on N_2: The total apparent capture cross section σ_c. PNT 62: Pivovar *et al.* (Ref. 17); ACM 56: Allison *et al.* (Ref. 18); NDFT 61: Nikolaev *et al.* (Ref. 19).

neutrals. This difference is also plotted in each of Figs. 10–13; for comparison there are shown also the total stripping cross sections of Allison[25] and of Barnett and Stier,[26] the total apparent stripping cross sections of Wittkower *et al.*[27] (for beams prepared in two different neutralizer gases), and the single-stripping cross sections of Pivovar *et al.*[28] It is immediately evident that the present results for σ_s are systematically higher than the quantities measured by each of the other investigators. It should first be noted that of these other results only those of Wittkower *et al.* represent measurements of precisely the same physical quantity that was measured in the present work. For incident He^0 the present total apparent stripping cross section σ_s is the sum of the single-stripping plus twice the double-stripping cross section, i.e.,

$$\sigma_s = \sum_{j=1}^{2} j\,({}_{00}\sigma_{jk}) .$$

(Recall that the unspecified subscript k denotes a summation over all values it can assume in the given gas.) In contrast, Allison and Barnett have measured the total attenuation of the neutral fast beam by both single and double stripping, with no attempt to distinguish these; hence, their result is simply

$$\sum_{j=1}^{2} {}_{00}\sigma_{jk} .$$

Finally, the data of Pivovar *et al.*, pertain only to ${}_{00}\sigma_{1k}$. While the results of Wittkower *et al.* represent nominally the same quantity as the present σ_s, these results were only relative measurements that were normalized to those of Stier and Barnett.[29] However, the disagreement with the present results cannot be accounted for in this fashion, because there are separate findings of Allison[30] and Solov'ev *et al.*,[23] which indicate that ${}_{00}\sigma_{2k}$ is not

TABLE III. Apparent cross sections for production of positive ions σ_+ and electrons σ_- by an incident beam of He^0. (All cross sections are in units of 10^{-16} cm^2/molecules.)

Projectile energy (keV)	Helium		Argon		Hydrogen		Nitrogen	
	σ_+	σ_-	σ_+	σ_-	σ_+	σ_-	σ_+	σ_-
150	1.22	2.51	8.47	13.1	2.64	4.23	8.18	13.7
180	1.26	2.56	8.37	13.4	2.72	4.45	7.98	13.7
200	1.26	2.56	7.95	13.1	2.66	4.39	7.82	13.8
250	1.27	2.55	7.85	13.5	2.50	4.17	7.52	13.7
300	1.22	2.47	7.52	13.3	2.40	4.03	7.45	13.7
350	1.20	2.40	7.33	13.2	2.26	3.84	7.20	13.5
400	1.14	2.28	6.91	12.7	2.16	3.68	6.82	12.9
500	1.05	2.09	6.34	12.0	1.93	3.32	6.50	12.5
600	0.99	1.95	6.00	11.4	1.75	3.01	6.05	11.9
700	0.91	1.81	5.36	10.5	1.56	2.68	5.62	10.9
800	0.86	1.68	5.05	9.76	1.40	2.42	5.25	10.4
900	0.79	1.56	4.85	9.25	1.30	2.24	4.98	10.1
1000	0.73	1.43	4.26	8.24	1.17	2.01	4.60	9.46

more than five percent of $_{00}\sigma_{1k}$. From this finding it follows that the quantities measured by the various investigators should not differ from each other, or from the present σ_S, by more than ten percent. Evidently, some other explanation must be sought for the present discrepancies, which are several times that large.

As was discussed previously, a major concern in this experiment is the possibility that the fast neutral beam might be appreciably contaminated with atoms in metastable excited states. If there were indeed an appreciable fraction of metastable excited atoms in the He^0 beam, it would be expected that this fraction, and therefore, their effects on the measured cross sections should vary with the pressure and with the nature of the gas used in the charge-exchange cell. A search for

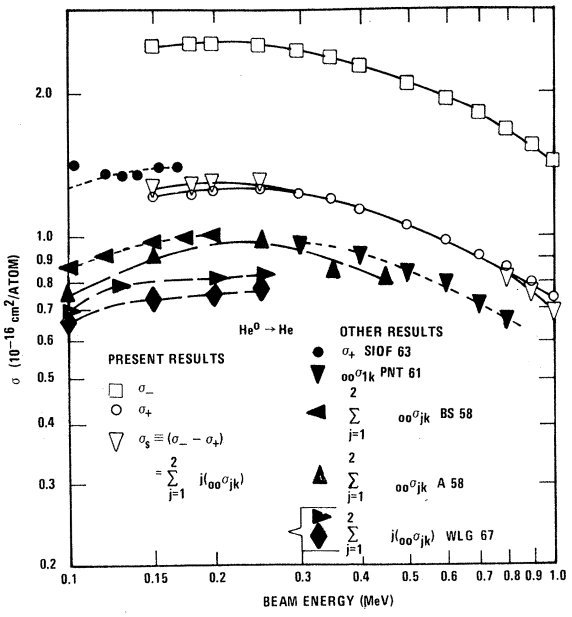

FIG. 10. He^0 atoms incident on He: The total apparent cross sections for the production of positive ions σ_+, free electrons σ_-, and the total apparent stripping cross section σ_S. SIOF 63: Solov'ev *et al.* (Ref. 23); PTN 61: Pivovar *et al.* (Ref. 28); BS 58: Barnett and Stier (Ref. 26); A 58: Allison (Ref. 25); WLG 67: Wittkower *et al.* (Ref. 27). (Upper curve with H_2 neutralizer gas, lower curve with He.)

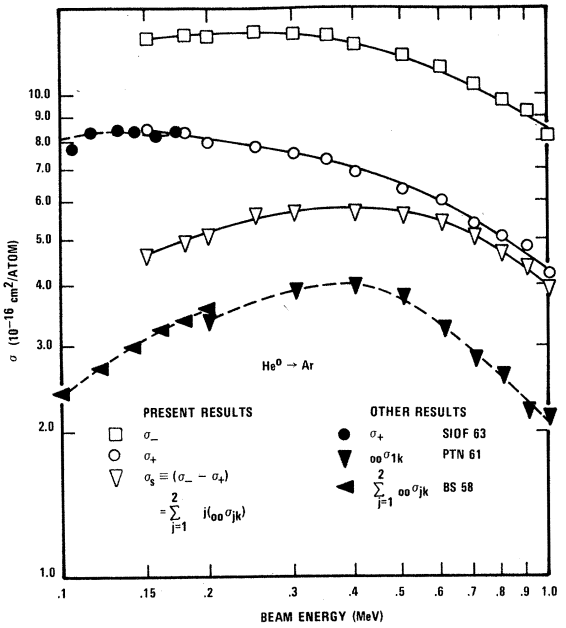

FIG. 11. He^0 atoms incident on Ar: The total apparent cross sections for the production of positive ions σ_+, electrons σ_-, and the total apparent stripping cross section σ_S. SIOF 63: Solov'ev *et al.* (Ref. 23); PTN 61: Pivovar *et al.* (Ref. 28); BS 58: Barnett and Stier (Ref. 26).

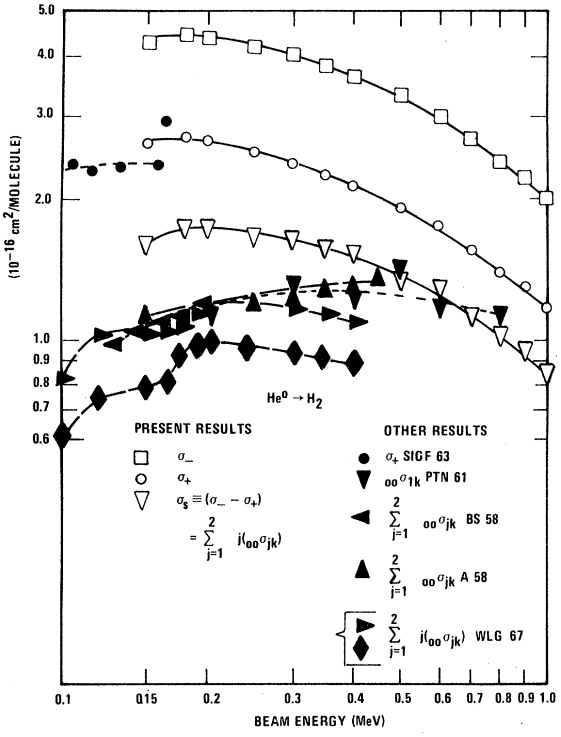

FIG. 12. He^0 atoms incident on H_2: The total apparent cross sections for the production of positive ions σ_+, free electrons σ_-, and the total apparent stripping cross section σ_S. SIOF 63: Solov'ev *et al.* (Ref. 23); PTN 61: Pivovar *et al.* (Ref. 28); BS 58: Barnett and Stier (Ref. 26); A 58: Allison (Ref. 25); WLG 67: Wittkower *et al.* (Ref. 27). (Upper curve with H_2 neutralizer gas, lower curve with He.)

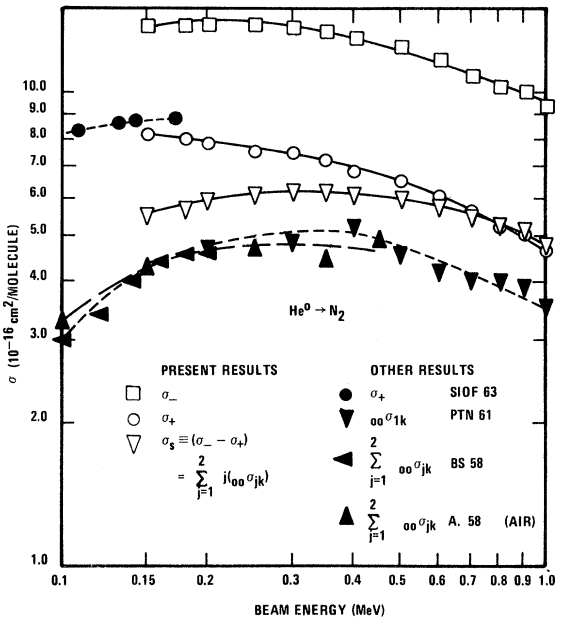

FIG. 13. He^0 atoms incident on N_2: The total apparent cross sections for the production of positive ions σ_+, free electrons σ_-, and the total apparent stripping cross section σ_S. SIOF: Solov'ev *et al.* (Ref. 23); PTN 61: Pivovar *et al.* (Ref. 28); BS 58: Barnett and Stier (Ref. 26); A58: Allison (Ref. 25).

such a dependence was made by observing the cross section values obtained for He^0 projectiles incident upon the target gases of H_2 and N_2. During these tests He and N_2 were used as neutralizer gases, and their pressures were varied over the range from 0.1 to more than 70 μ. In the 31-cm-long gas cell of this apparatus these pressures corresponded to neutralizer gas thicknesses of from 3.1 to 2170 μ cm. The results were that the measured cross section values in both target gases remained unchanged within a five percent scatter when the neutralizer gases were interchanged and when their pressures were varied over the entire pressure range used. As a result of these findings He was selected as the neutralizer gas, because of its high fractional yield of neutral beams, and was used for all of the neutral helium data reported in this work.

Further indications of the absence of appreciable numbers of excited states in the He^0 beam may be seen in the data of Fig. 10, for He^0 beams incident on He target gas. Since the target and projectile particles are both He^0 in this case, the cross sections for the total apparent ionization of the target and for the total apparent stripping of the projectile should be equal, provided that both collision partners are in the same initial atomic state. The latter is surely the ground state for the room temperature target-gas atoms. It is evident in Fig. 10 that $(\sigma_- - \sigma_+)$ and σ_+ are in fact equal within the experimental errors, and with only small deviations from complete agreement which are probably not significant.

This evidence for the absence of appreciable excited states in the He^0 beam is in agreement with the results of Allison.[25] However, it conflicts with the results of Barnett *et al.*[26] and of Wittkower *et al.*[27] who found evidence of the effects of excited states. In particular, Barnett and Wittkower observed that the cross sections decreased to an equilibrium value as the neutralizer gas pressure was increased. Furthermore, it was found that the equilibrium values varied, depending upon the selection of the neutralizer gas. However, the variation in gas cell pressure utilized in the present experiment covered an even greater range than either Barnett or Wittkower used, and it did not produce any change in the observed cross sections. Our conclusion was that the effects of excited states were unimportant in the present investigation.

In attempting to reconcile this discrepancy, it is perhaps important to consider the possibility that the distribution of excited states produced by the ion source may permit excited ions to reach

the neutralizer gas cell. If this were the case, a substantial number of collisions might be required to produce equilibrium in the fraction of excited states, as well as in the charge-state fractions. Furthermore, it is important to note that the flight distance from the neutralizer cell to the target gas was approximately 20 times longer in the present experiment than was the case in the apparatus of Wittkower *et al.*[27] The shorter this distance, of course, the greater the probability that normal excited states of the beam will not decay before reaching the collision region. Such differences in the source conditions and flight paths of the apparatuses might give rise to the observed effects.

2. H^0 *Atom Beams*

In contrast to the situation with He^0 beams, it is expected[31] that any atoms in the H^0 beam emerging from the gas cell in the 2*s* metastable state would be quenched by the electric field of the electrostatic analyzer. In support of this assumption it was observed that the cross-section values did not change as the analyzer field was varied from about 500 V/cm to more than 4000 V/cm. It was, therefore, concluded that H^0 metastables were fully quenched and therefore, were not important in the present measurements.

In Table IV and Figs. 14 – 17 are shown the total apparent ion production cross sections σ_+ and the total apparent electron production cross sections σ_- for H^0 incident on He, Ar, H_2, and N_2, respectively. As in the case of He^0, $\sigma_C = 0$ for incident H^0, so from Eqs. (12) and (14), $\sigma_+ = \sigma_i$, and the difference $(\sigma_- - \sigma_+)$ = the apparent stripping cross section σ_S. This cross section is also shown in the figures.

It should be noted that the energy range over which an H^0 beam of satisfactory intensity could be obtained was restricted to 150 to 400 keV. This restriction was due to the very rapid fall-off of the electron capture cross section of H^+ with increasing energy.

Shown for comparison in Figs. 14–17 are the measurements of Solov'ev *et al.*[32] for σ_+ and $(\sigma_- - \sigma_+)$, in which the stated maximum errors were ±15%. The σ_S cross-section measurements of Barnett and Reynolds,[8] and of Williams[33] are also shown for comparison. It is seen that their values, which are stated to have less than ±10% error, fall between the present results and those of Solov'ev, in both absolute value and energy dependence.

For the target gases helium and hydrogen (Figs. 14 and 16), a comparison is also made with a theoretical calculation of σ_S. Figure 14 shows the Bates and Williams[34] calculation of σ_S using the full Born approximation for the reaction

$$H(1s) + He(1s^2) \rightarrow H^+ + e + \sum_{n'l',n''l''} He(n'l',n''l''),$$

in which the summation includes an integration over the continuum. This calculated σ_S falls between the present result and Barnett's result and it is well within the error limits of both of these experiments.

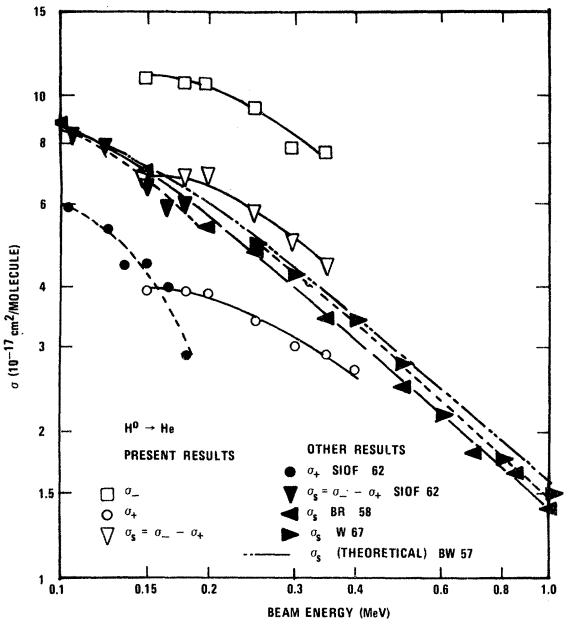

FIG. 14. H^0 atoms incident on He: The total apparent cross sections for the production of positive ions σ_+, free electrons σ_-, and the total stripping cross section σ_S. SIOF 62: Solov'ev *et al.* (Ref. 32); BR 58: Barnett and Reynolds, (Ref. 8); W 67: Williams (Ref. 33); BW 57: Bates and Williams (Ref. 34).

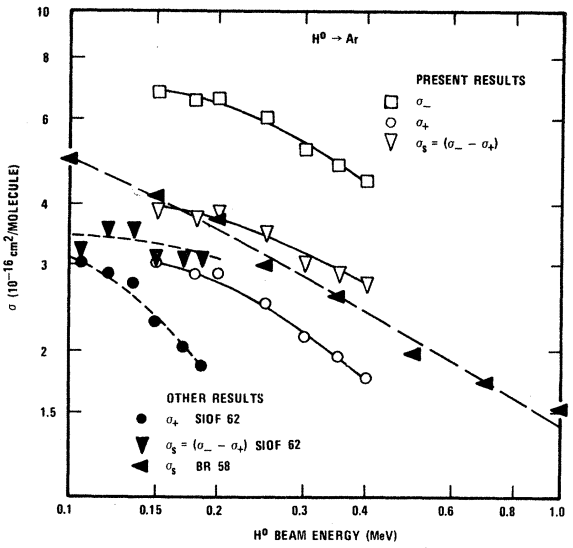

FIG. 15. H^0 atoms incident on Ar: The total apparent cross sections for the production of positive ions σ_+, free electrons σ_-, and the total stripping cross section σ_S. SIOF 62: Solov'ev *et al.* (Ref. 32); BR 58: Barnett and Reynolds (Ref. 8).

Table 4. Apparent cross sections for production of positive ions σ_+ and electrons σ_- by an incident beam of H^0. (All cross sections are in units of 10^{-16} cm^2/molecule.)

Projectile energy (keV)	Helium		Argon		Hydrogen		Nitrogen	
	σ_+	σ_-	σ_+	σ_-	σ_+	σ_-	σ_+	σ_-
150	0.40	1.1	3.0	6.9	0.91	1.9	3.0	6.6
180	0.39	1.1	2.9	6.6	0.85	1.7	2.8	6.1
200	0.39	1.0	2.9	6.7	0.82	1.6	2.7	6.2
250	0.35	0.95	2.5	6.0	0.71	1.4	2.2	5.3
300	0.31	0.80	2.1	5.2	0.62	1.2	1.9	4.5
350	0.29	0.75	1.9	4.8	0.54	1.1	1.9	4.5
400	0.27	• • •	1.8	4.6	0.50	1.0	1.7	4.3

A comparison is also shown in Fig. 16 with a result derived from the Bates and Griffing[35] calculation of σ_i, using the full Born approximation, for the ionization of the atomic target H^0 by incident neutral H^0,

$$H(1s) + H(1s) \rightarrow \sum_{nl} H(nl) + H^+ + e. \qquad (16)$$

The stripping of the atomic projectile by the atomic target would, obviously, have the same cross section. In this investigation, the target is, however, molecular hydrogen H_2. It is reasonable to suppose, however, that in the stripping reaction a hydrogen target molecule is approximately equivalent to two hydrogen atoms. Therefore, for comparison with the present σ_S results the calculated values for the atomic target have been multiplied by a factor of two. It is seen that this scaling procedure yields a cross section that is only slightly greater than the present experimental values for σ_S, but is substantially greater than the results of Barnett *et al.*[8] However, the uncertainty in the validity of this scaling procedure does not allow any firm conclusion that the present results are in better agreement with theory than are those of Barnett.

The same calculation could, of course, be compared with the experimental σ_i results. However, a different scaling procedure[1] from the atomic to the molecular target that takes account of the increased binding energy of the electrons in the

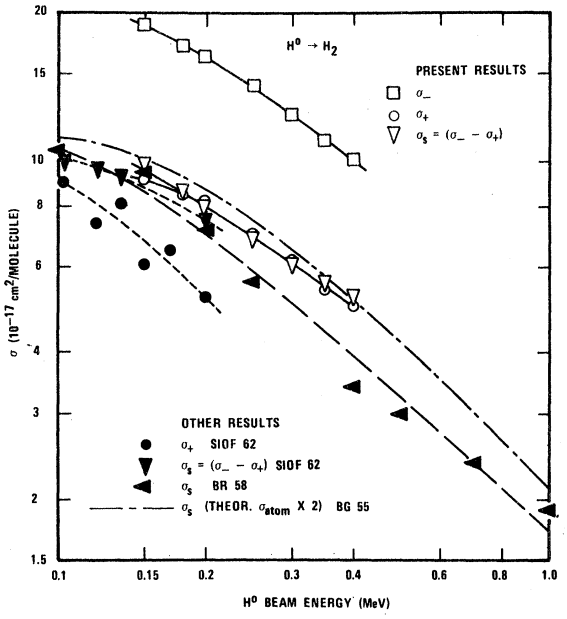

FIG. 16. H^0 atoms incident on H_2: The total apparent cross sections for the production of positive ions σ_+, free electrons σ_-, and the total stripping cross section σ_S. SIOF 62: Solov'ev *et al.* (Ref. 32); BR 58: Barnett and Reynolds (Ref. 8); BG 55: Bates and Griffing (Ref. 35).

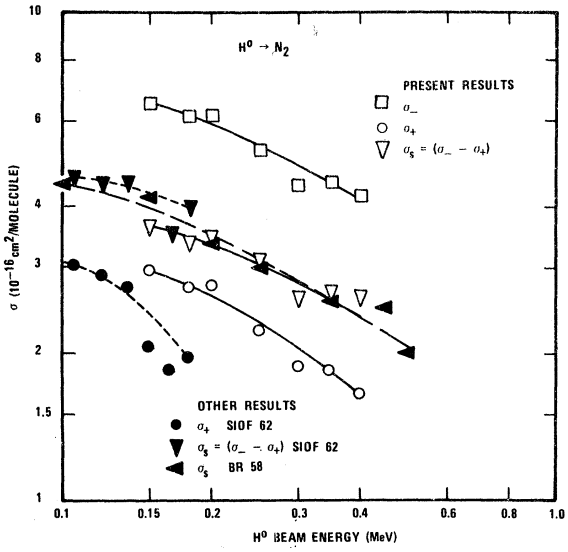

FIG. 17. H^0 atoms incident on N_2: The total apparent cross sections for the production of positive ions σ_+, free electrons σ_-, and the total stripping cross section σ_S. SIOF 62: Solov'ev *et al.* (Ref. 32); BR 58: Barnett and Reynolds (Ref. 8).

molecule, might be expected to hold. This comparison is discussed in Sec. IV. Remarkably, the present experimental results for σ_i and σ_S are seen to be equal in H_2 (except for a slight divergence at the lowest energies) which is not expected from the discussion above. The results of Solov'ev are not in agreement with this finding.

IV. SYSTEMATICS OF SIMPLE IONIZATION

In this section are presented systematic comparisons of the present experimental apparent ionization cross sections σ_i for incident He^{++}, He^0, and H^0 with one another, with previously published results for incident H^+ and He^+ in the same targets, and with the available theoretical calculations. These comparisons are suggested by the general form of the theory for high energies, and represent an extension of a previously published comparison[4] to include the present results. The present extended and more reliable results for incident He^{++} supplant the previously published results for this projectile.

Calculations of simple ionization cross sections in the full Born approximation have been made for only a few of the simplest cases. Among these are included the two calculations previously related, in Sec. III, to the stripping cross sections σ_S for H^0 incident on He^0 [Eq. (15)] and on H^0 [Eq. (16)]. As previously mentioned in Sec. III, these calculations can be applied to either the stripping of H^0 incident on targets of He and H^0, or conversely, to the ionization of the target H^0 by incident He^0 and H^0, respectively. Other available cases of interest include H^+ incident on H^0,[36] and on H^0,[37] He^+ incident on H^0,[38] and He^{++} incident on He.[39]

To extend the comparisons with theory to more of the cases investigated experimentally, it is useful to consider the Bethe approximation[4,40–42] which gives as an asymptotic limit to the full Born approximation for high energies the following general expression for ionization by a point charge projectile

$$\sigma_i = AZ^2(M/E)\ln(BE/M), \tag{17}$$

where E is the kinetic energy of the incident ion, Ze is its net charge and M is its mass in amu. The constants A and B should be characteristic of the target molecule and should not depend on the nature or the energy of the incident ion. An empirical evaluation of A and B for a given target molecule, from experimental measurements of σ_i for any one type of projectile can be used with Eq. (17); first, to extrapolate the measured σ_i for the given target molecule and projectile to energies outside the experimental range, in particular to higher energies, and, second, to estimate σ_i for the given target molecule and some other projectile with a different value of Z and/or M. Both types of applications of Eq. (17) will be employed in the present comparisons.

It should first be noted that the quantities M and E appear in Eq. (17) only in the ratio E/M, so that the expression predicts that various projectiles of equal Z but different M will have equal cross sections for equal velocities. This is a well known feature of the theory, which is also displayed by the full Born approximation.[36,40,41] It must next be emphasized that Eq. (17) applies only to the cross sections for simple single-ionization events, in which the projectile ion suffers no change in its charge state. The present apparent ionization cross sections σ_i do contain some contributions from other classes of events [see, for example Eq. (6) of Sec. I], but the total contribution from such events should be small. In addition Eq. (17) applies, strictly speaking, only to point charge projectiles, i.e., to electrons or bare nuclei. An incident ion carrying bound electrons might, however, be expected to be roughly equivalent in the simple ionization process to a partially screened point charge having an "effective" charge of Ze lying somewhere between its actual net charge and its nuclear charge. The value of Z for a given ion that is not a point charge, and indeed the validity of the whole concept of an effective projectile charge in ionization, can for the present be evaluated only by experimental test. The concept will be useful only if Z for a given projectile can be shown to be independent of the target molecule type and of the collision energy, or at least asymptotically so at high energies.

In summary, the cross section comparisons to be made among the various projectile particles and with the available theory will involve three relatively distinct aspects: (1) comparison for various projectiles on a given target between cross sections that are predicted to be equal when suitably scaled to equal projectile charge and velocity; (2) comparison of cross sections which are extrapolated beyond the energy range of the measurements by means of Eq. (17), with empirical values for the constants A and B; and (3) comparison for a given projectile in various targets of the apparent effective charge of the projectile. In some of these cases, the expected agreements may be found to be good with respect to the energy dependence of the cross sections, even when there are some disagreements with respect to absolute magnitudes.

In Figs. 18–21 the total apparent ionization cross sections σ_i for He^{++}, He^0, and H^0 in the target gases hydrogen, helium, argon, and nitrogen are plotted together with the previously published results[3,4] for H^+ and He^+ that were measured in this laboratory. (In all cases, the present results for He^{++} supplant the less extensive early results that were included in the previously published comparisons.) The energy axis is shifted a factor of four, in accordance with Eq. (17), to compare

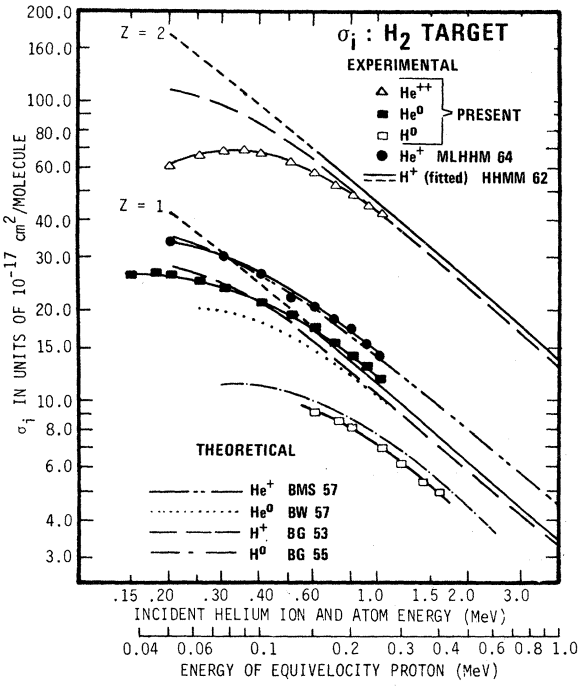

FIG. 18. Total apparent ionization cross sections for H and He ions and atoms incident on hydrogen. MLHHM 64: Martin *et al.* (Ref. 4); HHMM 62: Hooper *et al.* (Ref. 3). [Plots of Eq. (17) of text, with constant A and B chosen to fit the $Z=1$ curve to experimental proton results. The solid portion of this curve represents the actual proton data, while the dashed portion is an extrapolation outside the energy range of the data]; BMS 57: Boyd *et al.* (Ref. 38); BW 57: Bates and Williams (Ref. 34); BG 53: Bates and Griffing (Ref. 36) ($Z=1$: published curve for incident protons; $Z=2$: same curve $\times 4$, for comparison with He^{++} results); BG 55: Bates and Griffing (Ref. 35).

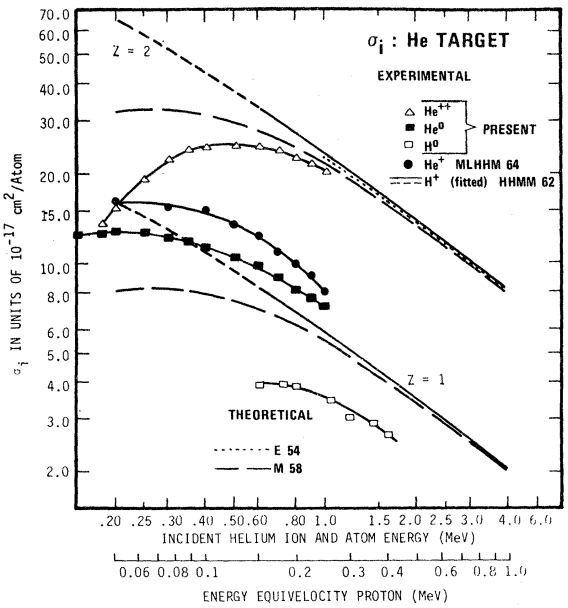

FIG. 19. Total apparent ionization cross sections for H and He ions and atoms incident on helium. MLHHM 64: Martin *et al.* (Ref. 4); HHMM 62: Hooper *et al.* (Ref. 3). [Plots of Eq. (17) of text, with constants A and B chosen to fit the $Z=1$ curve to experimental proton results. The solid portion of this curve represents the actual proton data, while the dashed portion is an extrapolation outside the energy range of the data]; E 54: Erskine (Ref. 39); M 58: Mapleton (Ref. 37) ($Z=1$: published curve for incident protons; $Z=2$: same curve $\times 4$, for comparison with He^{++} results).

the hydrogen and helium projectiles of equal velocity. Also shown in Figs. 18–21 are all of the available and relevant theoretical calculations mentioned previously.

In order to compare the experimental results on molecular hydrogen targets (Fig. 18) with the theoretical predictions, which are all for targets of atomic hydrogen, a scaling procedure was employed. This procedure, suggested by Bates and Griffing[36] and discussed by Hooper *et al.*,[3] allows for the difference in ionization potential between the atomic and molecular targets, and it was applied by Hooper to the theory for incident H^+ included in Fig. 18 as the curve labeled BG53. The solid portion of the $Z=1$ curves labeled HHMM 62 in Fig. 18 (as in Figs. 19–21) corresponds to a direct plot of Hooper's proton results, the dashed portion of the same curve is an extrapolation outside the data range by means of Eq. (17). As previously noted,[3] the portion of the curve corresponding to the actual proton data is in very good agreement with the theory with regard to energy dependence, and disagrees by only 10% in absolute magnitude. The extrapolation of the experimental proton results to energies below the experimental range diverges quite sharply from the theory, however, and is probably of very limited usefulness (which does not at all affect the probable validity of a similar extrapolation to energies above the experimental range).

The scaling procedure used for the preceding comparisons strictly applies only to a point charge projectile ion with no bound electrons. For projectiles with bound electrons, there are more terms in the interaction and the form of the dependence of the results on the projectile energy and ionization potential is consequently more complex.[36] It is therefore not self-evident that the same simple scaling procedure should have any validity. Nevertheless, it was tried for He^+, He^0, and H^0 projectiles, and for the case of He^+ incident on H_2 good agreement was obtained. This previously presented result is included in Fig. 18. The curve labeled BMS 57 represents a theoretical calculation for He^+ incident on H^0, scaled to H_2 as previously discussed, and the agreement with the estimated experimental ionization cross sec-

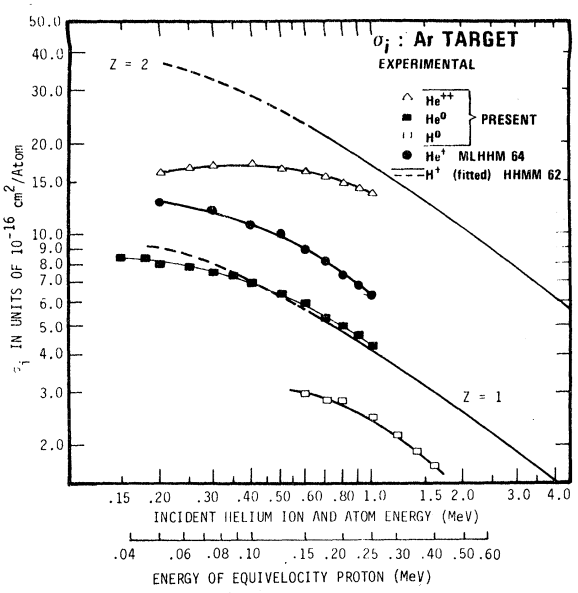

FIG. 20. Total apparent ionization cross sections for H and He ions and atoms incident on argon. MLHHM 64: Martin *et al.* (Ref. 4); HHMM 62: Hooper *et al.* (Ref. 3). [Plots of Eq. (17) of text, with constants A and B chosen to fit the $Z=1$ curve to experimental proton results. The solid portion of the curve represents the actual proton data, while the dashed portion is an extrapolation outside the energy range of the data.]

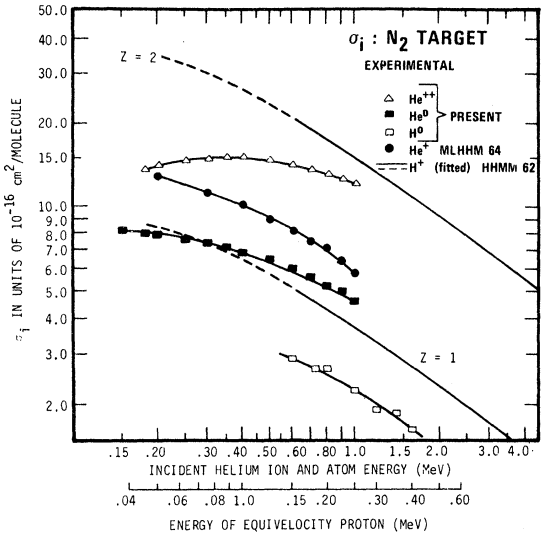

FIG. 21. Total apparent ionization cross sections for H and He ions and atoms incident on nitrogen. MLHHM 64: Martin *et al.* (Ref. 4); HHMM 62: Hooper *et al.* (Ref. 3). [Plots of Eq. (17) of text, with constants A and B chosen to fit the $Z=1$ curve to experimental proton results. The solid portion of the curve represents the actual proton data, while the dashed portion is an extrapolation outside the energy range of the data.]

tion is excellent. However, this agreement should be regarded with some reservation because the evaluation of σ_i for the He^+ projectile is complicated by the fact that the projectile can undergo both electron capture and stripping reactions. It was therefore necessary to estimate the relative sizes of several cross sections contributing to the directly measured σ_+ and σ_-, in order to arrive at an estimate[4] of σ_i.

The theoretical calculations for He^0 and H^0 incident on H^0, scaled to H_2 targets in the above manner, however, were found to be lower than the corresponding experimental values by about 30 and 50%, respectively, and so these results are not shown in the figure. Instead, the results obtained by simply doubling the theoretical atomic cross sections are presented, and these are seen to be in substantially better agreement with the experimental values. The curve in Fig. 18 labeled BG 55 represents the theoretical results for H^0 incident on H^0, multiplied by a factor of two. It is seen to lie about ten percent above the measured values and to have essentially the same energy dependence. Also shown in this figure is the theoretical calculation for He^0 incident on H^0, multiplied by a factor of 2 and labeled BW 57. This curve runs about 14% below the measured values, but in the upper part of the energy range the theoretical and experimental results have about the same energy dependence.

No explicit calculation is available in this energy range for He^{++} incident on hydrogen. However, the form of Eq. (17) predicts that the proton cross sections, multiplied by $Z^2=(2)^2$, and scaled to be equivelocity with He^{++}, should be equal to the He^{++} cross section for sufficiently high velocity. The HHMM 62 curve in Fig. 18 labeled $Z=2$ represents the experimental proton results (and their extrapolations) scaled in this manner. It is observed that the He^{++} results demonstrate quite precisely the expected behavior, i.e., they are just four times the proton results, for the higher energies used in this experiment. Also scaled in the same manner is the theoretical calculation for H^+ incident on H^0, scaled to H_2. It is also seen to provide good agreement with the observed values at the highest energies used in this investigation.

In Figs. 19–21, the same types of experimental curves as in Fig. 18 are shown, for the target gases He, Ar, and N_2. In each case the solid portion of the "$Z=1$, HHMM 62" curve is a direct plot of the experimental results for protons, while the dashed portion of the same curve is the extrapolation of these proton results using Eq. (17). The "$Z=2$, HHMM 62" curve is the above curve multiplied by 4, for comparison with He^{++} measurements.

In Fig. 19 the curves labeled E54 and M58 are explicit calculations for incident He^{++} and H^+, respectively. The energy range of the present experimental results for He^{++} do not overlap the

calculation of Erskine, except at 1.0 MeV, but at this point the agreement is good. Both of the curves for incident protons, scaled according to Eq. (17) and labeled $Z=2$, are seen to be approaching good agreement with the He^{++} results at the highest energies.

For the heavier target gases, argon and nitrogen, shown in Figs. 20 and 21, respectively, there are no explicit theoretical calculations available. It is seen that the He^{++} results appear to be approaching agreement with the scaled proton results at some higher energy, perhaps 2 or 3 MeV.

The final comparison to be made with these measurement is to determine whether or not the concept of the effective charge for ionization is valid for the non-point charge projectiles. The requirements for this concept to be valid for a given projectile are (1) that the cross sections for the given projectile have the same energy dependence as those of the true point charge projectiles such as H^+ or He^{++} (or at least asymptotically so at high energies), and (2) that the factor by which its cross sections differ from those of, say H^+, be the same for all target gases.

A comparison of the He^+, H^0, and He^0 results with the H^+ results in Figs. 18–21 indicates that (a) in all four cases, the previously measured He^+ curves become parallel to, and are roughly about a factor of 1.5 above the H^+ curves in at least the upper third of the energy range covered; (b) the H^0 curves also become parallel to the H^+ curves, and lie uniformly below them by about a factor of 0.64 in the upper energy range; (c) the He^0 curves, although they do become parallel to the H^+ curves toward higher energies, have no consistent factor between them that is independent of the target. Specifically the He^0 curves are approximately equal to the H^+ curves for both hydrogen and argon, which happen to be the lightest and heaviest targets, but are about a factor of 1.2 above the H^+ results for the other two cases. This amount of variation is outside of the estimated error limits for the He^0 measurements, and the variation is not systematically related to the target characteristics in any obvious way.

It appears, therefore, that He^+ and H^0 projectiles can be assigned effective charges for simple ionization, according to Eq. (17), of $\sqrt{1.5}=1.2$, and $\sqrt{0.64}=0.80$, respectively. However, the effective charge concept does not appear to be applicable to the He^0 projectile.

V. CONCLUSIONS

The experimental values of the total apparent cross sections for production of ions, σ_+, and of electrons, σ_-, were measured for the cases of He^{++}, He^0, and H^0 incident on the target gases He, Ar, H_2, and N_2.

For the cases involving He^{++} projectiles, the only experimental comparison data that were available were total charge changing cross sections for the capture of electrons by the projectile, which were equivalent to the difference $(\sigma_+ - \sigma_-)$ in the present data. It was noted that the agreement was excellent, which provided a strong confirmation of the validity of both the apparent ion production and the total charge changing cross section measurements.

For the neutral atomic projectiles, tests were performed to detect changes in the cross sections which were expected to be produced by excited atoms in the beams. However, no evidence was found for excited beam atoms.

For the cases involving an atomic helium beam, experimental comparison data were available for σ_+ and were in reasonably good agreement. The present results for $(\sigma_- - \sigma_+)$ were seen to be about 40% greater than was expected from certain related results of the other investigators, which all involved the observation of the change in beam composition as it passed through the target gas.

It was concluded from the present results for σ_i that it was not possible to assign a target-independent "effective charge" for ionization to He^0, the charge of a hypothetical point-charge ion of the same mass, that has the same cross section for simple ionization at high energies.

The data for $(\sigma_- - \sigma_+)$ obtained for the H^0 projectile were usually in rather good agreement with the available experimental comparison data; however, the agreement of the present σ_+ cross sections with the comparison values varied considerably among the various target gases. Also, in some cases the present and comparison results for σ_+ displayed a considerably different energy dependence. Confidence in the present results for σ_+ was enhanced when it was noted that the H^0 ionization cross section $\sigma_i=\sigma_+$ was displaced by a constant factor of 0.64 from the corresponding cross sections for H^+, above about 300 keV, for all four target gases. This close correlation, although not expected *a priori*, would be highly unlikely to occur in all four target gases if there were serious random errors present in the results for the individual gases.

From the form of the cross section in the Bethe-Born approximation [Eq. (17)], this constant offset in the H^0 and H^+ ionization cross sections implied that the concept of an "effective charge" for ionization could be applied to the H^0 projectile. The value obtained for this effective charge was $0.80e$.

It is interesting to note that the "effective charge" concept was applicable to the hydrogen projectile H^0 and the hydrogenic projectile He^+ (for which the effective charge $1.2e$ has been obtained previously[4]), but that it was not deemed applicable to the He^0 projectile in this experiment. No explanation of this observation is offered at present.

It was observed that generally good agreement was obtained between the experimental and theoretical cross sections, even those that were scaled

from atomic to molecular hydrogen. It is concluded, therefore, that the theory pertaining to the high-energy cross sections measured in this work is substantially correct for relative velocities above about 5×10^6 m/sec (≈ 0.5 MeV hydrogen), and that in some cases the theory appears to be valid at even lower velocities.

ACKNOWLEDGMENTS

It is a pleasure to acknowledge the constructive suggestions of Professor E. W. Thomas concerning problems that arose during this investigation. Particular appreciation is due Dr. D. L. Albritton for his assistance with the computer code that was used to speed data reduction. The authors are grateful to J. W. Martin for operating the Van de Graaff during the bulk of these measurements.

---

*This work was partially supported by the Controlled Thermonuclear Research Program of the U. S. Atomic Energy Commission under Contract No. AT-(40-1)-2591. The text of this paper has been assigned the Atomic Energy Commission Document Number ORO-2591-36.

†Present address: Ballistic Measurements Laboratory, USA Ballistic Research Laboratories, Aberdeen Proving Ground, Maryland. The results presented herein constituted a portion of a thesis submitted by L. J. P. to the faculty of the Georgia Institute of Technology in partial fulfillment of the requirements for the degree of Doctor of Philosophy.

[1]J. W. Hooper, E. W. McDaniel, D. W. Martin, and D. S. Harmer, Phys. Rev. 121, 1123 (1961).

[2]R. A. Langley, D. W. Martin, D. S. Harmer, J. W. Hooper, and E. W. McDaniel, Phys. Rev. 136, A379 (1964).

[3]J. W. Hooper, D. S. Harmer, D. W. Martin, and E. W. McDaniel, Phys. Rev. 125, 2000 (1962).

[4]D. W. Martin, R. A. Langley, D. S. Harmer, J. W. Hooper, and E. W. McDaniel, Phys. Rev. 136, A385 (1964).

[5]J. B. Hasted, Physics of Atomic Collisions (Butterworths Scientific Publications Ltd., London 1964), Chap. 3.

[6]S. K. Allison, Rev. Mod. Phys. 30, 1137 (1958).

[7]L. J. Puckett, D. W. Martin, and G. O. Taylor, Georgia Institute of Technology, Technical Report No. ORO-2591-35, 1967 (unpublished).

[8]C. F. Barnett and H. K. Reynolds, Phys. Rev. 109, 355 (1958).

[9]W. Gaede, Ann. Physik 46, 357 (1915).

[10]E. W. Rothe, J. Vac. Sci. Technol. 1, 66 (1964).

[11]A. E. deVries and P. K. Rol, Vacuum 15, 135 (1965).

[12]T. Takaishi, Trans. Faraday Soc. 61, 840 (1965).

[13]N. G. Utterback and T. Griffith, Jr., Rev. Sci. Instr. 37, 866 (1966).

[14]E. W. Thomas, Annual Technical Status Report No. 2, Project B-2021 of the Georgia Institute of Technology, U. S. Atomic Energy Commission Contract No. AT-(40-1)-2591, 1966 (unpublished).

[15]R. J. Tunnicliff and J. A. Rees, Vacuum 17, 457 (1967).

[16]M. J. Fulton and M. H. Mittleman, Proc. Phys. Soc. (London) 87, 669 (1966).

[17]L. I. Pivovar, M. T. Novikov, and V. M. Tubaev, Zh. Eksperim. i Teor. Fiz. 42, 1490 (1962) [English transl.: Soviet Phys. – JETP 15, 1035 (1962)].

[18]S. K. Allison, J. Cuevas, and P. G. Murphy, Phys. Rev. 102, 1041 (1956).

[19]V. S. Nikolaev, I. S. Dmitriev, L. N. Fateeva, and Y. A. Teplova, Zh. Eksperim. i Teor. Fiz. 40, 989 (1961); [English transl.: Soviet Phys. – JETP 13, 695 (1961)].

[20]S. T. Butler and R. M. May, Phys. Rev. 137, A10 (1965).

[21]A. H. Gabriel and D. W. O. Heddle, Proc. Roy. Soc. (London) 258, 124 (1960).

[22]H. C. Brinkman and H. A. Kramers, Proc. Acad. Sci. Amsterdam 33, 973 (1930).

[23]E. S. Solov'ev, R. N. Il'in, V. A. Oparin, and N. V. Fedorenko, Zh. Eksperim i Teor. Fiz. 45, 496 (1963) [English transl.: Soviet Phys. – JETP 18, 342 (1964)].

[24]E. W. McDaniel, Collision Phenomena in Ionized Gases (John Wiley & Sons, Inc., New York, 1964), Chap. 8.

[25]S. K. Allison, Phys. Rev. 110, 670 (1958).

[26]C. F. Barnett and P. M. Stier, Phys. Rev. 109, 385 (1958).

[27]A. B. Wittkower, G. Levy and H. B. Gilbody, Proc. Phys. Soc. (London) 90, 581 (1967); 91, 862 (1967).

[28]L. I. Pivovar, V. M. Tubaev, and M. T. Novikov, Zh. Eksperim. i Teor. Fiz. 41, 26 (1961) [English transl.: Soviet Phys. – JETP 14, 20 (1962)].

[29]P. M. Stier and C. F. Barnett, Phys. Rev. 103, 896 (1956).

[30]S. K. Allison, Phys. Rev. 109, 76 (1958).

[31]D. Jaecks, B. Van Zyl, and R. Geballe, Phys. Rev. 137, A340 (1965).

[32]E. S. Solov'ev, R. N. Il'in, V. A. Oparin, and N. V. Fedorenko, Zh. Experim. i Teor. Fiz. 42, 659 (1962) [English transl.: Soviet Phys. – JETP 15, 459 (1962)].

[33]J. F. Williams, Phys. Rev. 157, 97 (1967).

[34]D. R. Bates and A. Williams, Proc. Phys. Soc. (London) 70, 306 (1957).

[35]D. R. Bates and G. W. Griffing, Proc. Phys. Soc. (London) 68, 90 (1955).

[36]D. R. Bates and G. Griffing, Proc. Phys. Soc. (London) A66, 961 (1953).

[37]R. A. Mapleton, Phys. Rev. 109, 1166 (1958).

[38]T. J. M. Boyd, B. L. Moiseiwitsch, and A. L. Stewart, Proc. Phys. Soc. (London) A70, 110 (1957).

[39]G. A. Erskine, Proc. Roy. Soc. (London) A224, 362 (1954).

[40]N. F. Mott and H. S. W. Massey, The Theory of Atomic Collisions (Oxford University Press, Oxford, 1952), 2nd

ed.; Atomic and Molecular Processes, edited by D. R. Bates (Academic Press, Inc., New York 1962); E. H. S. Burhop, in Quantum Theory, edited by D. R. Bates (Academic Press, Inc., New York 1961), Vol I; T. Y. Wu and T. Ohmura, Quantum Theory of Scattering (Prentice-Hall, Inc., Englewood Cliffs, New Jersey, 1962).

[41]E. W. McDaniel, Collision Phenomena in Ionized Gases (John Wiley & Sons, Inc., New York, 1964), Secs. 6-11-D and 6-16-A.

[42]H. A. Bethe, Ann. Physik 5, 325 (1930).